Theoretical and Applied Climatology (2021) 146:883–895
https://doi.org/10.1007/s00704-021-03765-z

ORIGINAL PAPER

Projected changes in winter-season wet days over the Himalayan region during 2020–2099

Srabanti Ballav[1] · Sandipan Mukherjee[2] · Vaibhav Gosavi[2] · Ashok P. Dimri[3]

Received: 2 April 2020 / Accepted: 20 August 2021 / Published online: 8 September 2021
© The Author(s), under exclusive licence to Springer-Verlag GmbH Austria, part of Springer Nature 2021

Abstract

The Northern Hemisphere winter-season wet day climatology is extremely important to hydrological and agricultural processes of the Himalayan region (HR). However, knowledge of expected changes in the winter-season wet day climatology under global warming is significantly limited. Hence, this study attempts to quantify the expected changes in winter-season wet day climatological patterns for HR during 2020–2099 in comparison to a baseline period of 1980–2000 under two different warming scenarios, these being representative concentration pathways 4.5 and 8.5 (RCP 4.5 and RCP 8.5). Five climate model products covering the southern Asian region were obtained from the Commonwealth Scientific and Industrial Research Organization initiated Coordinated Regional Climate Downscaling Experiment (CORDEX) of the World Climate Research Programme and used for this purpose. Model biases are estimated with respect to observations for a base line period of 1980–2000. Model ensemble non-linear trends of the winter-season wet days for the periods 2020–2040, 2041–2070, and 2071–2099 are estimated using Sen's slope estimator, while ensemble average future changes in the number of winter-season wet days are estimated, and attempts made to identify the topographical ranges that are expected to be mostly affected by the changing winter-season wet day climatology. The results show that the CORDEX-regional climate models have a positive bias, ranging between 1 and 30 days, across the high altitudes of the entire Himalayas, and model performance improves with an increasing number of wet days per season. Although the impact of stronger warming (i.e. under RCP 8.5) is noted to enhance the area averaged non-linear trend of wet days over northwestern (0.014) and eastern (0.005) Himalaya during 2071–2099, the model ensemble predicted area-averaged reduction in the frequency of wet days of 0.3 to 1.0 day is highly likely by the end of this century. It is also observed that the Himalayan region within the range of 1000–2500 m above sea level may experience a decline in winter-season wet days by up to 0.8 to 3.2 days under the warming scenarios of both RCP 4.5 and 8.5.

Keywords Winter-season wet days · Himalayan region · CORDEX

1 Introduction

The Himalayas, fresh water reservoir for most of the glacier-fed rivers of south and central Asia, are the life line of about 1.5 billion people of the world (Nandargi and Dhar 2011). Consequently, precipitation in the form of rain and snow over the region is a significant control of annual and inter annual variation of water resources, agro-horticultural production and hydroelectric power generation (Mall et al. 2006; Goyal et al. 2015; Kanwal et al. 2019). Since Himalayan topography plays a pivotal role controlling the precipitation patterns by blocking and modulating air circulation and the vertical stratification of the atmosphere, different precipitation regimes exist across the east-west and north-south stretches of the region (Chalise and Khanal 2001; Dimri and Niyogi 2013; Ghimire et al. 2015).

Over the northwestern Himalayan region, almost one-third of annual precipitation is received during winter (typically December to February, but often extending to April) as a result of eastward moving low pressure systems or extra-tropical cyclones termed 'Western Disturbances'

✉ Sandipan Mukherjee
sandipanmukherjee@hotmail.com

[1] Previously at Aryabhatta Research Institute of Observational Sciences (ARIES), Manora Peak, 263001, Nainital, Uttarakhand, India

[2] GB Pant National Institute of Himalayan Environment, Kosi-Katarmal, 263643, Almora, India

[3] School of Environmental Sciences, Jawaharlal Nehru University, 110067, New Delhi, India

that incorporate moisture convergence from both the Bay of Bengal and Arabian Sea (Hatwar et al. 2005; Dimri 2014). However, northeast India, representing the eastern Himalayas, including the Brahmaputra river basin and all seven Indian Himalayan states, receives rainfall from thunderstorms during early and late winter periods. The frequency of winter Western Disturbances related precipitation events over the northwestern Himalayan region is typically 6–7 for each month from December to April of which 2–3 cases may result in extreme precipitation (Pisharoty and Desai 1956; Dimri 2006). It has also been noted that a high frequency of 'El-Nino - Southern Oscillation' (ENSO) events can trigger higher numbers of monsoon 'breaks' but also higher precipitation during winter over the Himalayas. That is the northwest Indian winter precipitation is positively correlated with ENSO events (Dimri 2006; Yadav 2009), unlike the northwest Himalayan summer monsoon seasonal rainfall, which is negatively related to Nino 3.0 and 3.4 indices (Mukherjee et al. 2020). At the same time, it has also being noted by Dimri et al. (2015) that increased snow cover in Eurasia could push more depressions along the path of the southern winter jet bringing more winter precipitation to the northwestern Himalayas. The average winter-season rainfall over northwestern Himalayan region, particularly over Jammu and Kashmir, Himachal Pradesh and Uttarakhand, is reported to be $\sim$ 190, 130 and 210 mm, respectively (Nageshwararao et al. 2016). However, the effect of these eastward moving Western Disturbances over eastern Himalaya is negligible as this region receives around 2% of its rainfall in winter compared to the average annual rainfall of $\sim$ 2400 mm (Parthasarathy et al. 1994). Nonetheless, assessment of the intra-seasonal oscillations of winter-season rainfall along with the limit of predictability and determinism, as undertaken by Mukherjee et al. (2011, 2016); Mukherjee (2017) and Mukherjee (2021) for summer monsoon rainfall over Himalayas, are yet to be carried out.

In the current context of increasing surface air temperature around the world, the hydro-climatic processes of the Himalayas are also reported to have changed significantly over the last couple of decades (Dyurgerov and Meier 2005; Bhutiyani et al. 2007; Singh et al. 2011; IPCC 2014). Therefore, impacts of increasing air temperature on water and ecosystem resources of the Himalayas need to be assessed so that necessary adaptive measures can be drafted according to the COP-21 Paris agreement. Furthermore, different countries of the world have unequivocally agreed to keep the current global warming rate within 1.5–2°C by the end of this century under this agreement. Consequently, climate projection studies at a wide range of spatio-temporal scales are being increasingly used to develop various adaptation and mitigation practices. Since winter-season rainfall and wet days play an important role controlling hydro-ecological systems of the Himalayas, particularly for the northwestern Himalayas, a detailed future scenario-based assessment is expected to be beneficial for any adaptive measures. However, few studies of future climate projections over the Himalayas are carried out using global and regional climate models (Dash et al. 2012; Kulkarni et al. 2013; Ghimire et al. 2015; Mukherjee et al. 2019; Midhuna and Dimri 2019), and a comprehensive assessment of projected changes in winter-season wet days over Himalayas has not yet been carried out. Therefore, in order to adress this knowledge gap, this work evaluates the future state of winter-season wet days over Himalayas using CORDEX (Coordinated Regional Climate Downscaling Experiment) rainfall products, for the period 2020 - 2099, for the two representative concentration pathways 4.5 and 8.5 (RCP 4.5 and RCP 8.5).

2 Data description

Projected changes in the winter-season wet days over HR were estimated using data from the CORDEX South Asia experiment, simulated for regional scale climate change assessment up to the year 2099, by the Commonwealth Scientific and Industrial Research Organisation (CSIRO) using a Conformal Cubic Atmospheric Model (CCAM; McGregor and Dix 2001). Daily model products, having a grid size of 0.5° $\times$ 0.5°, from the following five experiments: ACCESS, GFDL, NoRESM, CNRM and MPI were used, and details of these experiments can be found in Mukherjee et al. (2019). The CORDEX programme included many experiments over South Asia wherein various global and regional climate models were used. The performances of these experiments widely varied over the Himalayan region primarily due to differences in the parameterizations used (Mishra 2015; Ghimire et al. 2015). However, the group of CSIRO South Asia simulations was one of a small number of experiments conducted using only one standard regional climate model, i.e. CCAM, for consistency in the downscaled products. As a consequence, irrespective of biases in the climatic parameters, the performance of all the CSIRO-CCAM experiments was mostly consistent over the Himalayas. Therefore, only the above mentioned five CORDEX-CSIRO experiments were considered in this study. The winter rainfall analyses were carried out for (i) two representative concentration pathways (RCPs) — RCP 4.5 and RCP 8.5, and (ii) three future periods: Y_1 representing years 2020 to 2040, Y_2 representing years 2041 to 2070, and Y_3 representing years 2071 to 2099. Biases in the daily model simulated rainfall were computed for a base line period 1980–2000, represented as Y_b, using APHRODITE gridded products (version APHRO_MA_V1101R2, Yatagai

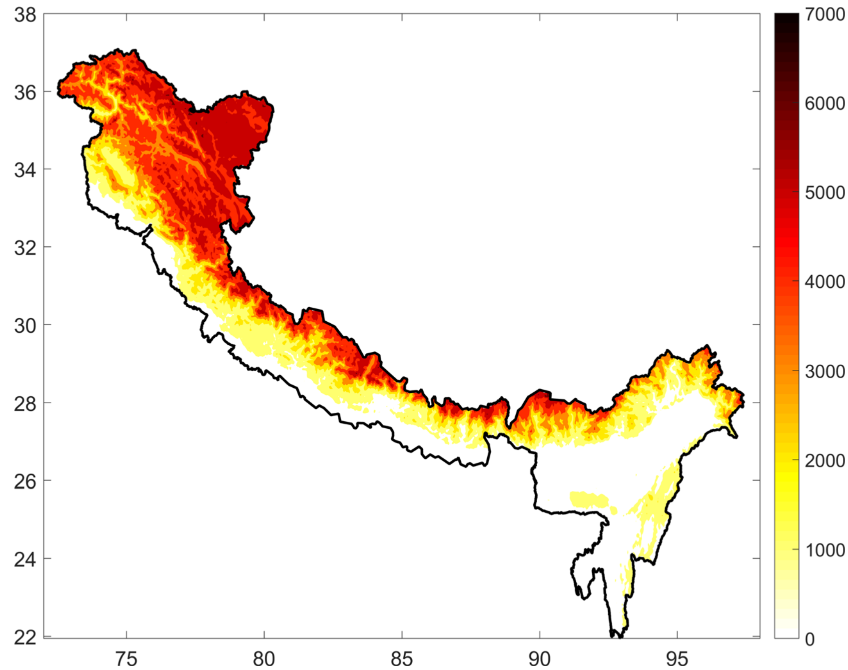

Fig. 1 The model domain with topographic elevation (m), estimated from SRTM digital elevation model 90 m data for the Himalayan region

et al. (2009, 2012)), termed here as 'observation' having a spatial resolution of 0.25° × 0.25°. Except for the GFDL experiment of RCP 4.5 during 1971–2099, all the model products were used to estimate ensemble average changes in winter-season wet days. The climatological analyses of this study were carried out over the geographical region 22–38° N and 72–98° E. The topography within this region is shown in Fig. 1. Topographic elevation (m) was estimated using Shuttle Radar Topography Mission (SRTM) digital elevation model data at 90 m spatial resolution. Specific domains for northwestern and eastern Himalayas were (i) 28–38° N, 72–82° E and (ii) 22–30° N, 88–98° E, respectively, were used for further analysis. The north-east of India is considered within the HR, as this region has many geological thrust features due to north and north-eastern movement of the Gondwana plate which collided with the Eurasian plate. The northeast Indian region is geographically intertwined with the Himalayan region through the Main Boundary Thrust (Dikshit and Dikshit 2014), while the Himalayan Main Boundary Thrust and the Naga-Disang Thrust separate the Himalayan terrain from the eastern hilly region via the Brahmaputra valley. Moreover, subtropical climate signatures are also observed in the mountainous regions of the north-east Himalayas where winter-season maximum air temperature varies between 10 and 15° and minimum temperature remains sub-zero.

Although a daily rainfall of 10 mm is categorized as 'light rainfall' during the Indian summer monsoon by the India Meteorological Department (Pattanaik and Rajeevan 2010), the standard definition of wet days during the winter-season has not been defined. Therefore, to determine a limit of rainfall for defining winter wet days over HR, the daily winter-season rainfall during 1980–2000 was estimated using APHRODITE data (Fig. 2). In order to define the winter-season wet days, a box plot of daily total rainfall, observed at each grid point for all the winter-seasons of 1980–2000, was produced (inset Fig. 2). It was noted that the 75^{th} percentile of the daily rainfall was 4.68 mm/day, whereas the mean daily rainfall was 4.32 mm/day. Therefore, the nearest integer of the 75^{th} percentile of daily rainfall, i.e. 5.0 mm/day, was set to be the limit for determining wet days. Consequently, those days having rainfall $\geq$ 5.0 mm/day were identified as wet days.

3 Methods

Before analysing the climatological changes of future period winter-season wet days, the climatology of wet days was investigated for the baseline period of 1980–2000 (Y_b) using APHRODITE data. The winter-season wet days were estimated by summing those days during January, February, November and December of a year when daily rainfall was greater or equal to 5.0 mm. The average model bias ($\overline{B}$) was computed by the following equation:

$$\overline{B} = \frac{1}{n}\sum_{1}^{n} rd_w^m - \frac{1}{n}\sum_{1}^{n} rd_w^o \quad (1)$$

Fig. 2 Observed averaged winter-season rainfall (mm/day) during 1980–2000. The inset figure represents a box plot of daily rainfall observed at each grid point for the all the winter seasons of 1980–2000 over the HR. The black rectangles are representing areas of north-western and eastern Himalayas considered for area averaged values

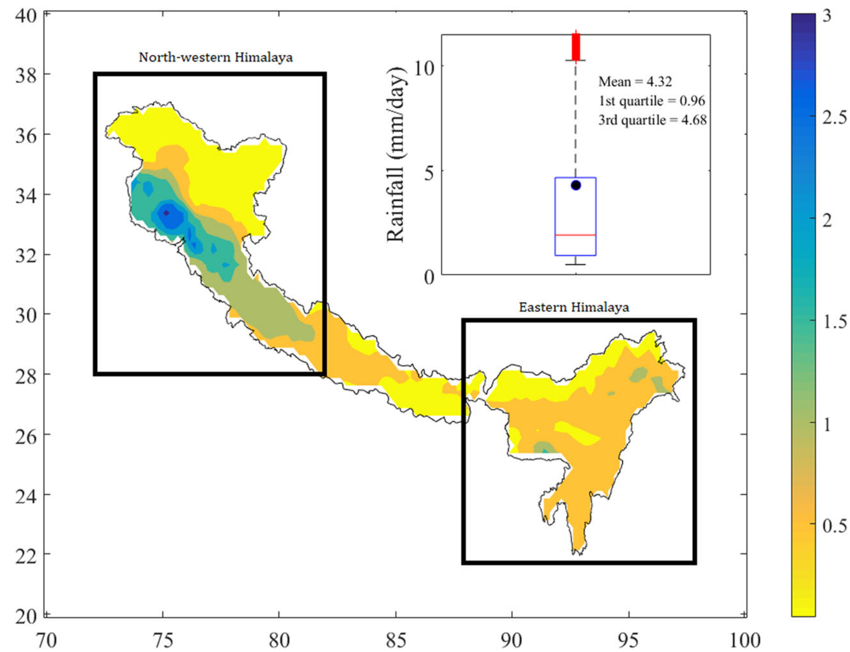

where n = 1980 to 2000 (21 years) and $rd_w^{m/o}$ represents modelled and observed total winter-season wet days, respectively. Similarly, the ensemble average bias ($\overline{\overline{B}}$) was estimated by computing the arithmetic average of all model biases.

Once the model biases were computed, trends in projected changes of the winter-season wet day climatology were estimated across the HR using the spatial non-parametric method of Sen's slope following Sen (1968). The Sen's slope method was used due to its advantage of being able to analyse non-linear time series having missing values and outliers. The winter-season wet days at each grid point were identified for individual models during 2020–2040 (Y_1), 2041–2070 (Y_2) and 2071–2099 (Y_3), and ensemble average winter-season wet days were derived for both warming scenarios (i.e. RCP 4.5 and 8.5). Finally, Sen's slope was estimated at each grid point at a 95% confidence level with a positive Sen's slope indicating an increasing trend, with a negative value depicting a decreasing trend in the time series. A detailed numerical description of the Sen's slope technique can be found in Mukherjee et al. (2015). Once the spatial pattern of Sen's slope was estimated for the three future periods, area averaged Sen's slope was computed for northwestern and eastern Himalayas.

Ensemble average changes in winter-season wet days for the three future periods ($\overline{\Delta rd_w^Y}$) were computed using the following equation:

$$\overline{\Delta rd_w^Y} = \frac{1}{m}\sum_1^m \left(\frac{1}{n}\sum_1^n rd_w^{Y_{1/2/3}} - \frac{1}{n}\sum_1^n rd_w^{Y_b}\right) \quad (2)$$

where m represents the number of models (i.e. five) and $rd_w^{Y_{1/2/3}}$ represents winter-season wet days simulated by each model for the future periods Y_1 to Y_3, respectively, and $rd_w^{Y_b}$ represents total winter-season wet days simulated by each model for baseline period 1980–2000. Once the spatial $\overline{\Delta rd_w^Y}$ values were estimated for the three future periods, area averaged $\overline{\Delta rd_w^Y}$ values were estimated for the northwestern and eastern Himalayas.

To estimate the statistical significance of spatially averaged changes in the number of winter-season wet days within the three future periods, two sample t-tests were carried out between the following pairs: $\overline{\Delta rd_w^{Y_1}} - \overline{\Delta rd_w^{Y_2}}$ and $\overline{\Delta rd_w^{Y_2}} - \overline{\Delta rd_w^{Y_3}}$ for the northwestern and eastern Himalayas under RCP 4.5 and 8.5, respectively. The null hypothesis "two independent random samples are normal-distributed with equal but unknown variances" was tested at confidence intervals (C.I.) of 95% and 75%.

In order to identify the topographic elevation ranges of Himalayas expected to be most impacted by the changing winter-season wet day climatology during 2021–2099, SRTM digital elevation model data at 90 m spatial resolution were used with $\overline{\Delta rd_w^Y}$. Since $\overline{\Delta rd_w^Y}$ values were obtained at a spatial scale of 0.5° × 0.5°, elevation data were extracted from the SRTM data for all those points within the HR for which latitude and longitude information of $\overline{\Delta rd_w^Y}$ were available. Finally, scatter diagrams between 500 m bin averaged elevation and $\overline{\Delta rd_w^Y}$ were produced. The exercise was carried out for all three future periods (i.e. Y_1 to Y_3) and two RCPs (i.e. RCP 4.5 and 8.5) over the northwestern and eastern Himalayas.

4 Results and discussion

4.1 Bias: winter-season wet day climatology

Numerical modelling of the climate processes over mountain terrain using global climate models is difficult due to the coarse resolution and insufficient parameterizations (Kumar et al. 2013; Dimri et al. 2018). On the other hand, regional climate models are better than global models as they can resolve small scale processes with the inclusion of subgrid scale topography, and better representation of atmosphere-hydroshpere-biosphere feedback processes (Giorgi and Bates 1989; Beniston 2003; Rummukainen 2010; Dimri et al. 2018). However, regional climate models are not yet fully capable of simulating climatic processes over mountain terrain due to very complex orographic-induced dynamical forcings. As a result, verification of regional climate products using available station data has revealed a general trend of cold and wet biases over mountains including the Himalayas (Giorgi et al. 2004; Solman et al. 2008; Maharana and Dimri 2014). Therefore, any conclusion regarding current and future states of climate over Himalayas, derived based on regional climate model products, requires a complete assessment of biases in the data. Consequently, to initially estimate ensemble average bias of CORDEX simulated products for winter-season wet days, mean wet days per winter-season during 1980–2000 were estimated using APHRODITE data (Fig. 3a). The mean wet days per winter-season were found to be maximum over the Kashmir valley and Himalayan foothills of Himachal

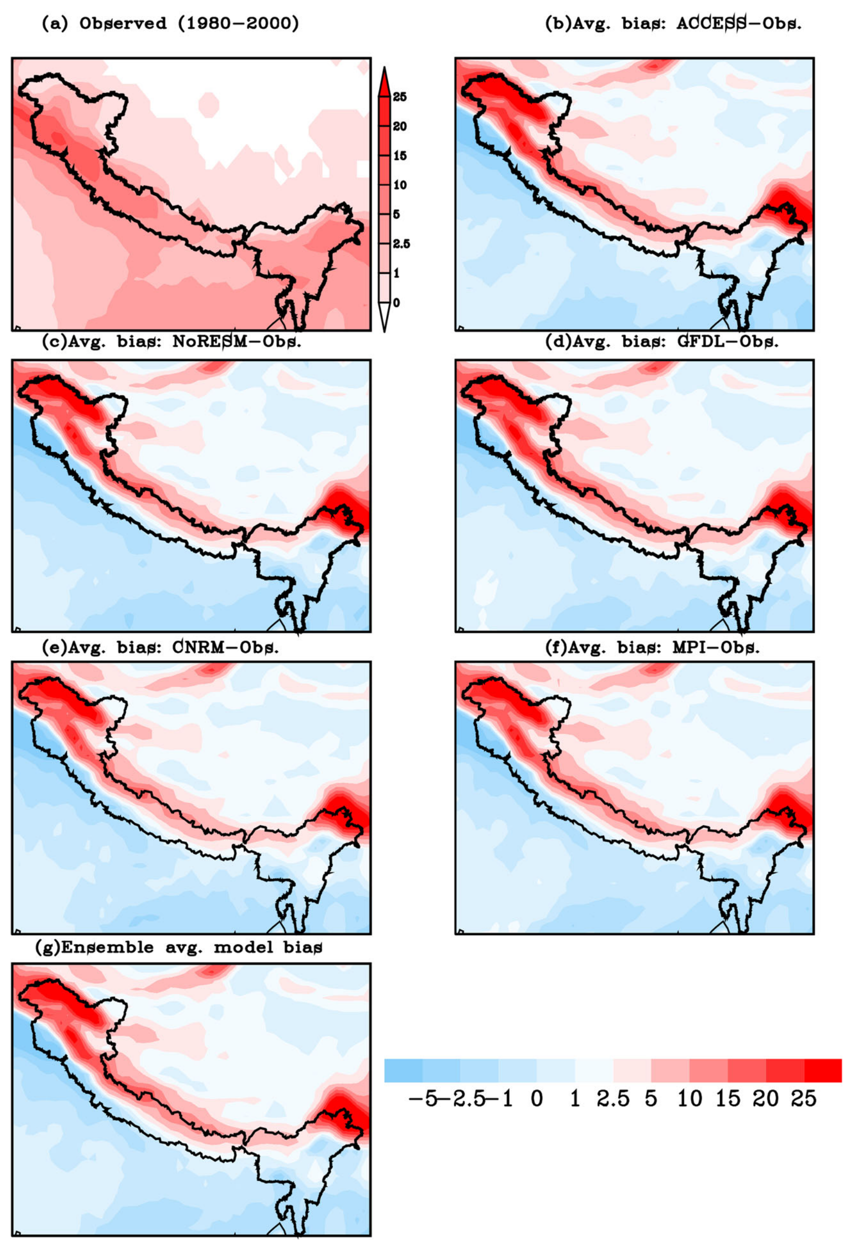

Fig. 3 Subplot (a) shows the distribution of observed mean wet days per winter-season during 1980–2000. Subplots (b-f) shows the average model bias ($\overline{B}$) in simulating mean wet days per winter-season during 1980–2000, whereas, subplot (g) shows the ensemble average bias ($\overline{\overline{B}}$) in simulating mean wet days per winter-season during 1980–2000. Geographical coordinates are similar to Fig. 1

Pradesh and Uttarkhand ranging between 10 and 30 days, whereas the hills of Arunachal Pradesh had an average of 2–10 number of wet days per season, predominantly from thunderstorms. The generic spatial distribution of model bias ($\overline{B}$) for all the selected CORDEX-RCMs was positive, ranging between 1 and 30 days, across the high altitudes of Himalayan regions, including the eastern Himalayas (Fig. 3b-f). It can also be noted from Fig. 3g that ensemble model performance improved over the central Himalayas, ranging from Nepal to Bhutan hills, where positive biases were within the range of 2.5–10 days. The positive biases, as indicated in Fig. 3a-g, were also found to be consistent with the earlier observations of Palazzi et al. (2013) and Mishra (2015) who noted wet biases over the foothills and higher elevations of the Himalayas with uncertainties between 30 and 100% for winter rainfall.

Monthly mean wet days per winter-season during the Y_b period, estimated using APHRODITE data, indicated that the winter-season wet day occurrence gradually increases from November to February as monthly mean wet days change from 0.7 (1.9) to 0.9 (2.2), 1.3 (2.4) and 1.9 (3.5) with values in parentheses representing maxima (Fig. 4). The monthly

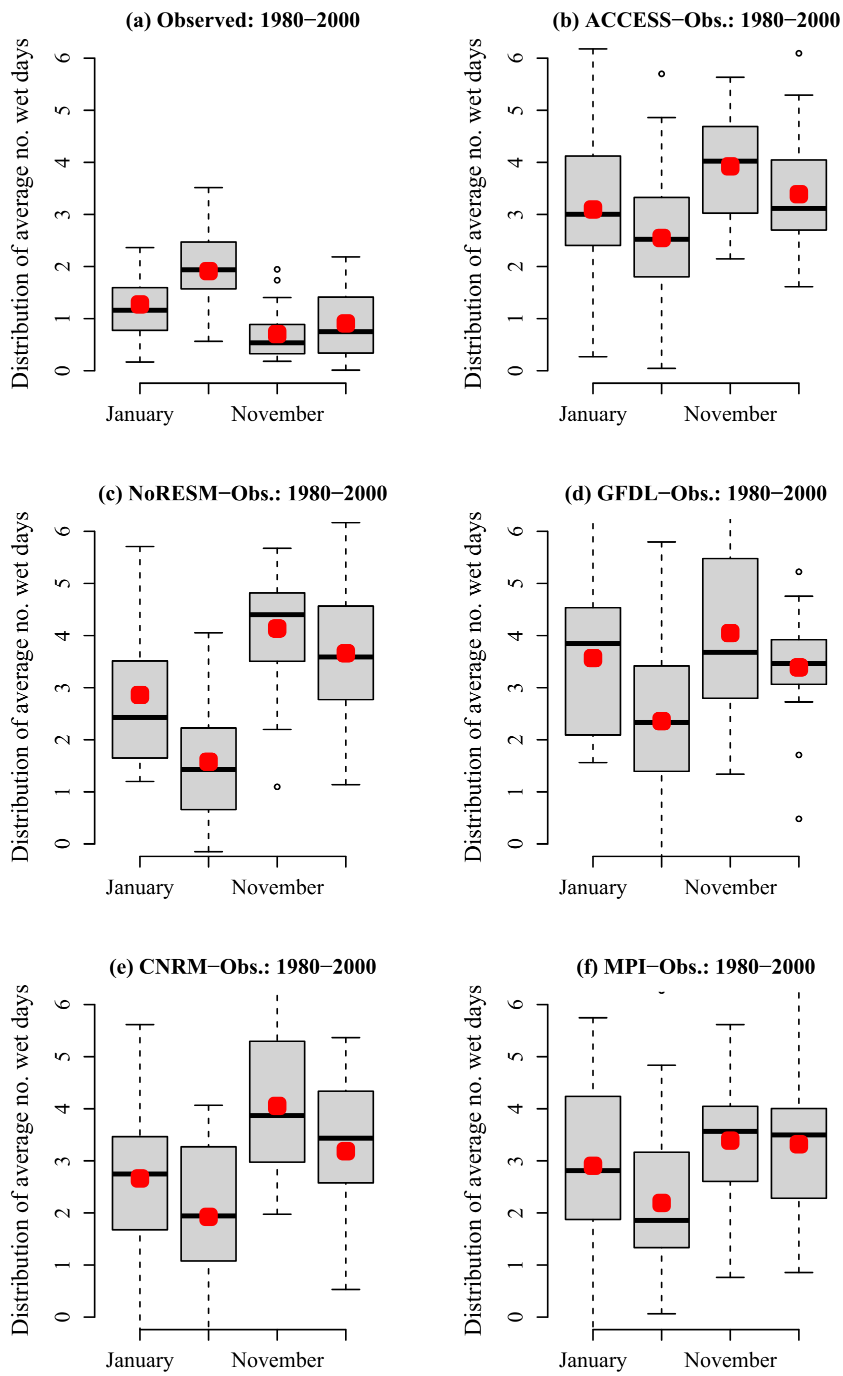

Fig. 4 Subplot (a) shows the observed (APHRODITE) monthly distribution of the total number of wet days per winter-season during 1980–2000 within the HR. Subplots (b–f) show the model bias in simulating the monthly distribution of the total number of wet days per winter-season during 1980–2000 within the HR

mean ensemble averages of model bias were 3.9, 3.4, 3.0, and 2.1, respectively, for November to February, indicating model performances improvement with increasing number of wet days. The month of November (February) had the highest (lowest) wet bias for all CORDEX models during the Y_b period. However, it should be noted that these estimated biases were not used for any bias correction, rather as indicated by Mukherjee et al. (2019), it is assumed that the model biases will be carried forward for future projections until 2099 under similar convective and cloud microphysical parameterizations. Hence, it is also assumed that the time-invariant model bias could effectively be insignificant when estimating differences in the number of occurrence of wet days per season for baseline and future periods.

4.2 Trends in the winter-season wet day climatology under a warmer climate

Results of the spatial non-parametric Sen's slope estimator analysis for identifying trends in the winter-season wet day climatology under RCP 4.5 and 8.5 and for three future periods (Y_1 to Y_3) are provided in Fig. 5. The non-parameteric Sen's slope values were estimated at each grid point at a 95% confidence level. The general observation from Fig. 5 is that the number of wet days over Jammu and Kashmir and high mountain areas of Uttarakhand and Nepal, as well as lower to middle Himalayas, are expected to reduce until 2070 under both RCP 4.5 warming. Interestingly, an overall positive trend in the wet days are expected for both RCP 4.5 and 8.5 scenarios towards the end of the century, i.e. 2071–2099, particularly over the eastern Himalayas. This increasing trend of wet days is in agreement with the ensemble area averaged Sen's slope value, presented in Fig. 6.

It can be noted from Fig. 6a that RCP 8.5 warming is expected to enhance the occurrence of wet days over the entire northwest Himalayas during Y_2 and Y_3 in comparison to RCP 4.5. The area averaged Sen's slope values (± standard deviation) during Y_2 and Y_3 over the northwest Himalayas were estimated to be − 0.01 (±0.075) and 0.014 (±0.04) in comparison to − 0.004 (±0.036) and 0.004 (±0.037), respectively, for the RCP 8.5 and 4.5 warming scenarios, respectively.

Similar to the northwestern Himalayas, it can be noted from Fig. 6b that RCP 8.5 warming is also expected to enhance occurrence of wet days over the entire eastern Himalayas during Y_2 and Y_3 in comparison to RCP 4.5. Moreover, the area averaged Sen's slope values of Y_2 and Y_3 over the eastern Himalayas, under both RCP 4.5 and 8.5 warming, showed positive trends. The area averaged Sen's slope values (± standard deviation) during Y_2 and Y_3 over eastern Himalayas were − 0.01 (±0.034) and 0.005 (±0.042) in comparison to − 0.025 (±0.039) and

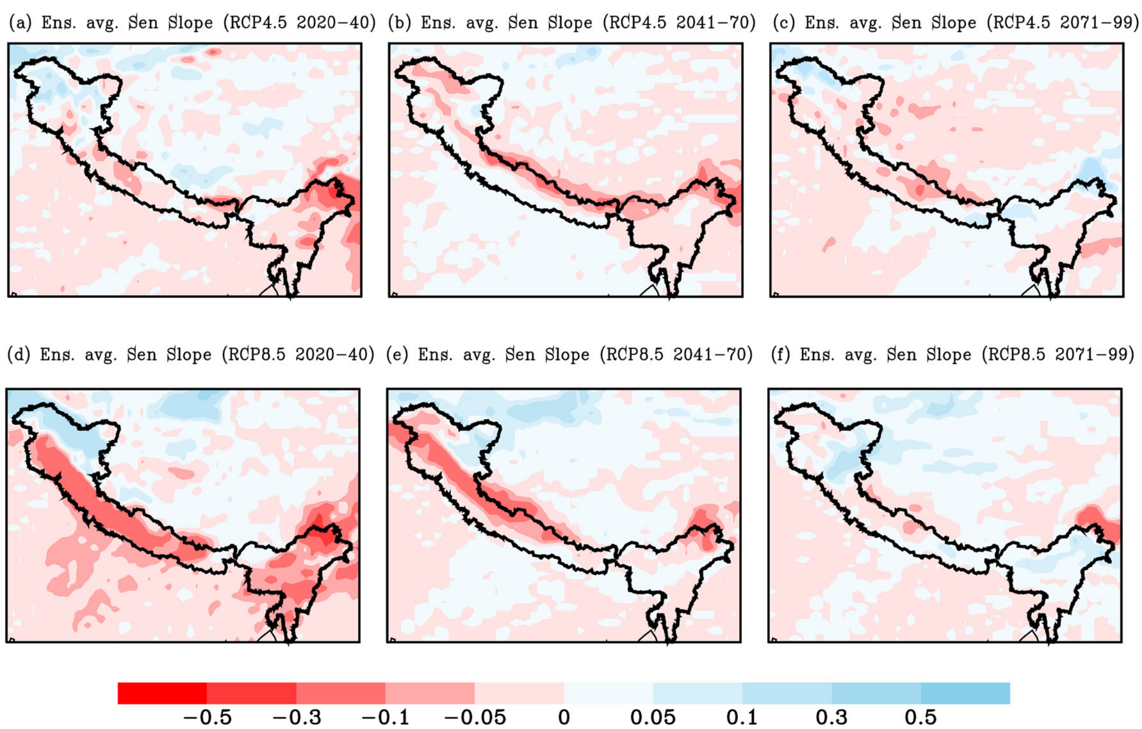

Fig. 5 Ensemble averaged Sen's slope values estimated for the number of winter-season wet days for (a–c) 2020–2040, 2041–2070, 2071–2099 under RCP 4.5, and (d–f) 2020–2040, 2041–2070, 2071–2099 under RCP 8.5, respectively. Geographical coordinates are similar to Fig. 1

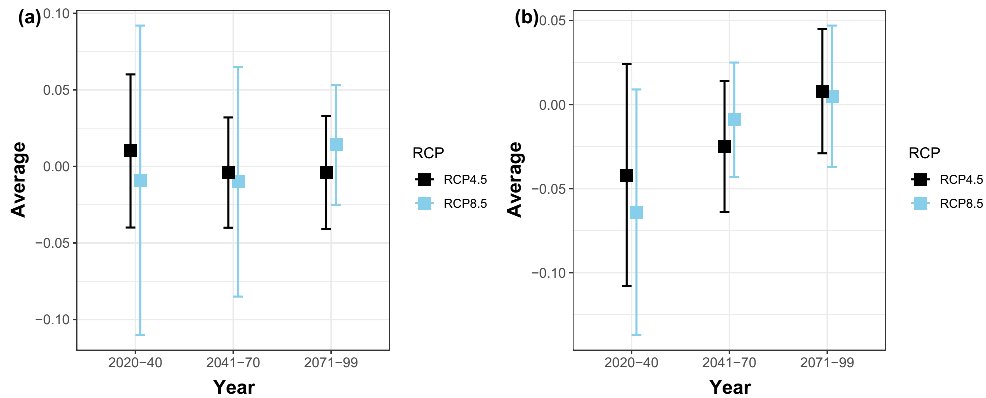

Fig. 6 Ensemble area averaged Sen's slope, represented as 'Average' in the y-axis label, estimated for the number of winter-season wet days for (a) northwestern and (b) eastern Himalayas, respectively

0.008 (±0.037), respectively, for RCP 8.5 and 4.5 warming scenarios.

Although the Sen's slope analysis of the wet day climatology may indicate that winter wet days are expected to increase under a warmer climate, true spatio-temporal changes in the winter-season wet day climatology may only be deduced once the future wet day climatology is compared with the base line period observations. Therefore, a detailed analysis of the ensemble average of expected changes in the number of winter-season wet days for three future periods with respect to a base line period is carried out in the following section.

4.3 Expected changes in the wet day climatology under warmer climate

The ensemble average expected changes in the winter-season wet days during three future periods ($\overline{\Delta rd_w^Y}$) are presented in Fig. 7. It can be noted from Fig. 7 that the Jammu and Kashmir valleys including mid to lower elevations of the Himachal Pradesh and Uttarakhand states of India are mostly expected to receive fewer winter wet days. The reduction of winter-season wet days over these regions may vary between 1 and 6 days under RCP 4.5 and 8.5 warming scenarios, indicating a reduction and/or inconsistent occurrence of western disturbances and associated precipitation. Similarly, the eastern Indian Himalayan states of Arunachal Pradesh and parts of northern Assam are expected to have reduction in winter wet day occurrence by more than 5 days. Since the impact of western disturbances over the eastern Himalayas is almost negligible, reduction in the occurrence of wet days for this region could be linked to lesser convective activity resulting in rainfall less than 5 mm/day. A closer inspection of Fig. 7 further reveals that the cold desert areas (such as the Ladakh and Himalayan territory bordering China) are expected to experience a rise in wet day occurrence by 1–4 days under both the warming scenarios, whereas the foothills of the northwest Himalayas are expected to receive fewer wet days. The maximum positive change in winter wet day occurrence (≥ 5 days) over the northwestern cold desert areas is anticipated during the 2071–2099 period under RCP 8.5. The aggressive warming in the RCP 8.5 scenario is also noted to increase the nonlinear trend of winter wet day occurrence, and is in agreement with the studies of Sanjay et al. (2017) and Midhuna and Dimri (2019) who reported enhancement in rainfall amounts, particularly for the northwestern Himalayas and Karakoram mountain range.

In order to assess the overall regional pattern of ensemble average expected changes in winter-season wet days, area averaged $\overline{\Delta rd_w^Y}$ values were produced for both RCP 4.5 and 8.5 scenarios and for Y_1 to Y_3 (Fig. 8). Over the northwestern Himalayas, where the winter-season rainfall is entirely dependent on Western Disturbances, mean (± standard deviation) values of $\overline{\Delta rd_w^Y}$ for Y_1 to Y_3 (Fig. 8a) under RCP 4.5 were noted to be − 0.02 (± 1.59), 0.3 (± 1.90) and − 0.22 (± 2.2), respectively. However, $\overline{\Delta rd_w^Y}$ values for Y_1 to Y_3 under RCP 8.5 were noted to be 0.73 (± 1.81), − 0.12 (± 2.62) and − 0.23 (± 3.99), respectively. From the area averaged values of $\overline{\Delta rd_w^Y}$ over the northwest Himalayas, it is apparent that the impact of consistent surface warming would reduce winter wet day occurrence. The number of winter wet days would particularly decline under the aggressive warming scenario of RCP 8.5. This reduction in winter wet day occurrence does not appear to contradict the earlier observations of Sanjay et al. (2017) and Midhuna and Dimri (2019) and with the increasing nonlinear trend of wet days reported here, this is probably due to an increase in rainfall amount but a reduction in the overall number of seasonal wet days.

For the eastern Himalayas, $\overline{\Delta rd_w^Y}$ for Y_1 to Y_3 (Fig. 8b) under RCP 4.5 was noted to be − 1.23 (± 1.34), − 1.08 (± 1.76) and − 1.43 (± 1.83), respectively. Similar values for RCP 8.5 were − 0.98 (± 1.61), − 1.88 (± 2.11) and − 1.42 (± 2.4), respectively. It can also be noticed that by the end of this century, inconsistencies in $\overline{\Delta rd_w^Y}$ for both RCP 4.5 and 8.5 would be at a maximum over the entire Himalayas

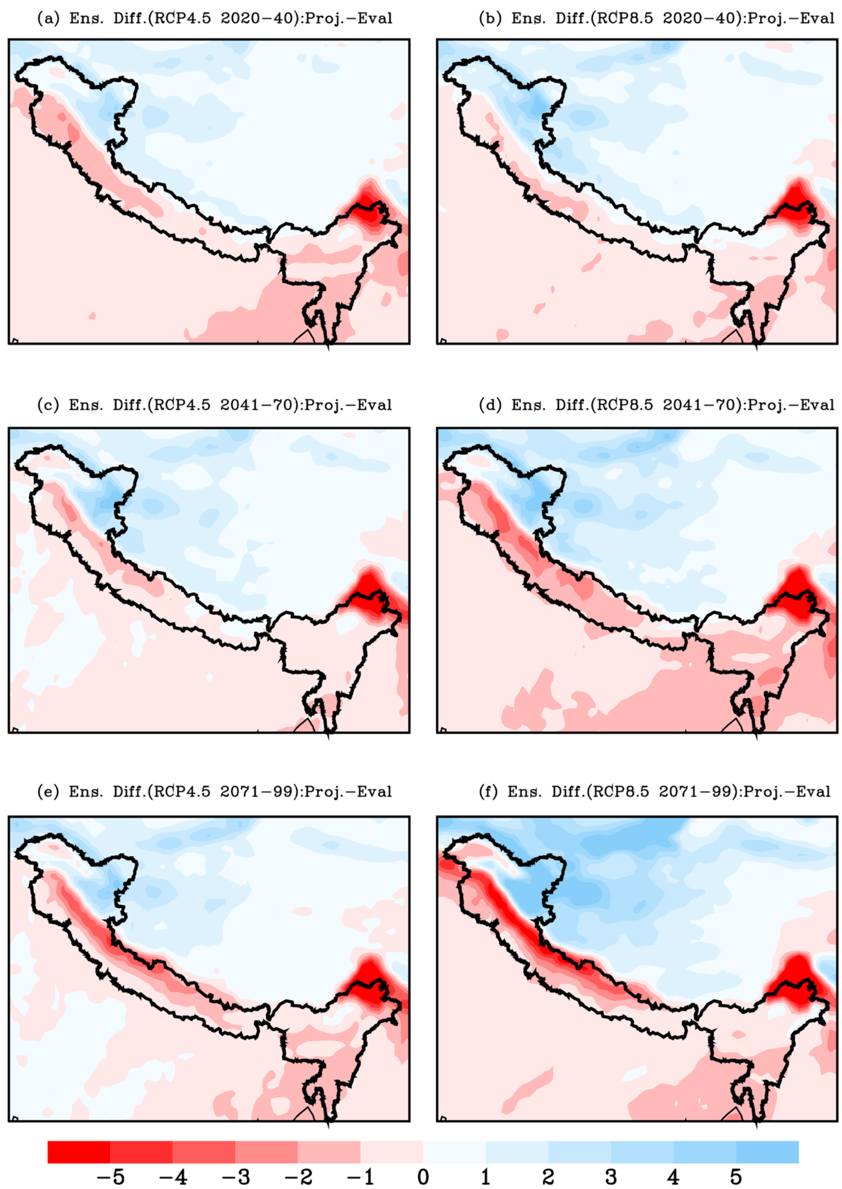

Fig. 7 Ensemble averaged expected changes in the number of winter-season wet days ($\overline{\Delta rd_w^Y}$) under (a, c, e) RCP 4.5 and (b, d, f) RCP 8.5 during (a, b) 2020–2040, (c, d) 2041–2070, and (e, f) 2071–2099 with respect to the evaluation period 1980–2000. Geographical coordinates are similar to Fig. 1

as standard deviations of $\overline{\Delta rd_w^Y}$ were highest during 2071–2099 under both warming scenarios. The interesting feature of these changes in $\overline{\Delta rd_w^Y}$ is the comparatively higher impact of warming on declining wet day occurrence over the eastern Himalayas in comparison to the northwestern Himalayas as the decline in $\overline{\Delta rd_w^Y}$ remains at < 0.3 days in

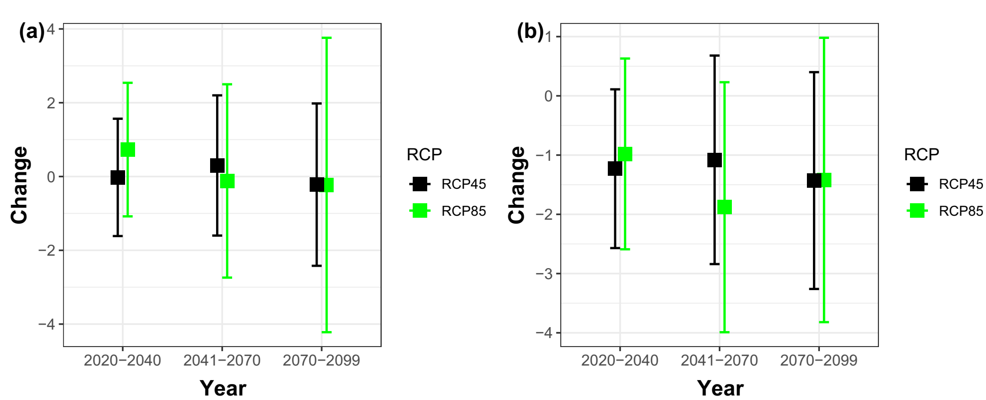

Fig. 8 Ensemble area averaged future changes in the number of winter-season wet days ($\overline{\Delta rd_w^Y}$) under RCP 4.5 and 8.5 warming scenarios during 2020–2099 over (a) the north-western Himalayas and (b) the eastern Himalayas with respect to the evaluation period 1980–2000

Table 1 The two sample *t*-tests between spatially averaged changes in the number of winter-season wet days within the three future periods (Y_1 to Y_3) for both RCP 4.5 and 8.5 and northwestern (NWH) and the eastern Himalayas (EH), respectively

Himalayan region	Case	RCP	T-stat	Rejection of H0 at 95% C.I.	Rejection of H0 At 75% C.I.
NWH	2020–40 and 2041–70	4.5	−1.53	N	Y
NWH	2041–70 and 2071–99	4.5	2.09	Y	Y
NWH	2020–40 and 2041–70	8.5	3.13	N	N
NWH	2041–70 and 2071–99	8.5	0.27	Y	Y
EH	2020–40 and 2041–70	4.5	−0.68	N	Y
EH	2041–70 and 2071–99	4.5	1.43	N	Y
EH	2020–40 and 2041–70	8.5	3.54	N	N
EH	2041–70 and 2071–99	8.5	−1.51	Y	Y

comparison to < 1.0 days in the eastern Himalayas. Results of this study are found to be similar to Wiltshire (2014) who reported that the impact of warming on future glacier mass balance decline would be higher in eastern Himalayas compared to the northwestern Himalayas. Although there is no definitive proof of tele-connections between the occurrence of Western Disturbances over the northwest Himalayas and winter time convective storms resulting in higher precipitation over eastern Himalayas, the larger impact of declining wet days over the eastern Himalayas with an increasingly warm atmosphere could be related to the changing dynamics of convective storms over this region under erratic behaviour of the Western Disturbances. Although the above-mentioned statement is in line with observations made by Pohl et al. (2017) over South Africa, detailed assessment of this hypothesis is yet to be made over HR, particularly in the context of changing moisture flux.

Results of the two sample *t*-tests, carried out between spatially averaged changes in the number of winter-season wet days during Y_1 to Y_3 for RCP 4.5 and 8.5 in the northwestern and eastern Himalayas, are provided in Table 1. Since rejection of the null hypothesis at the 95% confidence interval would indicate the average difference between samples has high confidence, it can be concluded that projected changes in the winter-season wet days over the northwestern Himalayan region are very likely to occur during 2070–2099 (Y_3) in comparison to 2041–2070 (Y_2) for both RCP 4.5 and 8.5 warming scenarios. Consequently, it is expected that the increasing warming is very likely to reduce winter-season wet days over the northwestern Himalayas. However, in the case of the eastern Himalayan region, rejection of the null hypothesis at the 95% confidence interval was only noted between 2041–2070 (Y_2) and 2071–2099 (Y_3) under the RCP 8.5 scenario, indicating that the eastern Himalayas is also very likely to receive fewer winter-season wet days during 2071–2099 (Y_3) in comparison to 2041–2070 (Y_2).

4.4 Expected changes in wet day climatology under warmer climate with respect to elevation

Dhar and Rakhecha (1981) and Bookhagen and Burbank (2006) reported that the monsoon rainfall over the central Himalayas occurs predominantly over two elevation zones, one at around 800 masl and the other at around 2200 masl. Subsequently, it was reported by Mukherjee et al. (2016) that dominant modes of monsoon intra seasonal oscillations are also concentrated at around 747.9 m and 2227.2 m over the northwestern Himalayas and around 1200 m over the eastern Himalayas. However, knowledge of such dominant elevation zones within the Himalayas receiving higher rainfall during the winter-season is limited. Therefore, in order to estimate the impact of expected changes in winter-season wet days with topographic elevation over the Himalayas under warming scenarios, scatter diagrams between 500 m bin-averaged elevation and $\overline{\Delta rd_w^Y}$ were produced (Fig. 9).

It can be noted from Fig. 9a–b that over the northwestern Himalayas, winter-season wet days are expected to increase above 3500 m elevation through out the period 2020 to 2099 irrespective of warming scenario, and the average enhancement of wet day occurrence is likely to be > 2 days with respect to the Y_b period. Similarly, over the eastern Himalayas (Fig. 9c–d), although winter-season wet day occurrence is expected to increase above 3000 m elevation under both warming scenarios, the over all change is expected to be < 1 day with respect to the Y_b period. That is, in spite of the anticipated enhancement of wet day occurrence under the warming scenarios, the net change in wet day frequency with respect to elevation would remain negative. However, it is to be noted that CORDEX-RCM biases, as estimated in this study in Section 4.1, were also positive across the high altitudes of HR, hence, change in the values of winter-season wet day occurrence over high elevations may differ during a bias corrected appraisal.

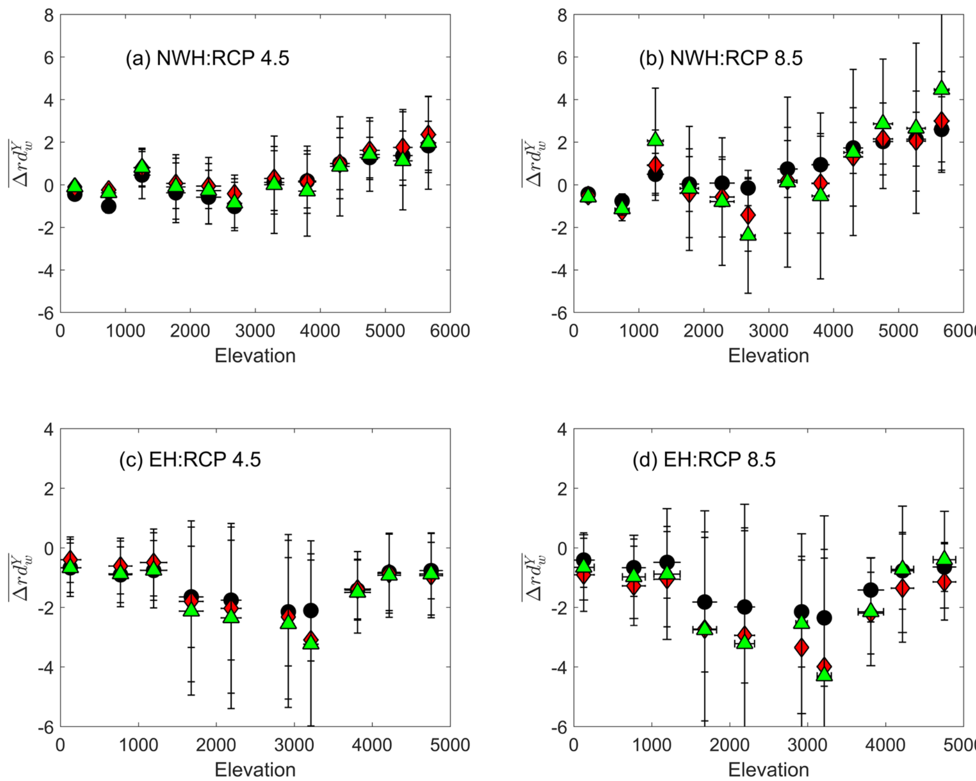

Fig. 9 500 m bin averaged elevation frequency distributions of ensemble averaged expected changes in the number of winter-season wet days for three future periods ($\overline{\Delta rd_w^Y}$) are represented for (a–b) the northwestern and (c–d) eastern Himalayas under RCP 4.5 and 8.5, respectively. The black circles, red diamonds, and green triangles represent averages for future periods Y_1 to Y_3, respectively. Vertical and horizontal bars are standard deviations

The future warming scenarios are expected to result in a decline in winter wet day occurrence over the mid-altitude regions (i.e. 1000–2500 m above sea level) of both the northwestern and eastern Himalayas. The average decline in wet day occurrence over the mid-altitude regions of the northwestern Himalayas is expected to vary between 0.8 and − 0.8 day under RCP 4.5, and between 2.0 and − 2.4 days under RCP 8.5 during Y_1 to Y_3. Similarly, average decline in wet day occurrence over the mid-altitude regions of eastern Himalayas is expected to vary between − 0.6 and − 2.3 days under RCP 4.5, and between − 0.6 and − 3.2 days under RCP 8.5. These findings imply that the mid-altitudes of both the northwestern and eastern Himalayas are expected to experience a higher decline in wet days under the aggressive warming of RCP 8.5.

5 Summary and conclusion

This study has aimed to assess the impact of future warming on expected changes in the winter-season wet day patterns over the HR for the period 2020–2099. Two different warming scenarios, RCP 4.5 and 8.5, were considered in this study. Ensemble averages of winter-season wet days were derived from five climate model products of the CSIRO, Australia, initiated by CORDEX of the World Climate Research Programme over the South Asia region.

The spatial distribution of model biases for winter-season wet day occurrence, as estimated for a base line period of 1980–2000, indicated that CORDEX-RCMs had positive biases, ranging between 1 and 30 days within a season, primarily across the high altitudes of HR (elevation ≥ 3000 m). The ensemble model bias was also noted to be lowest during the month of February (2.1 days). Individual CORDEX model performance was noted to improve with increasing number of wet days per season.

Comparison of the number of winter-season wet days between the baseline (1980–2000) and future periods (2020–2099) clearly indicated that wet day occurrence is expected to decrease for the entire Himalayan region. However, it can also be concluded that stronger warming of the RCP 8.5 scenario may result in a marginally higher wet day frequency over the HR than for the RCP 4.5 scenario. It could further be concluded from this study that the Himalayan region with elevations of 1000–2500 masl would experience the highest decline in wet day occurrence under the warming trend. However, the present study did not include any assessment of changes in the occurrence of extreme rainfall events over the HR during the winter-season. As a result, this research could followed up by a separate assessment of future changes in winter-season extreme rainfall events over the Himalayas to provide a more comprehensive appraisal.

Acknowledgements The World Climate Research Programme's Working Group on Regional Climate, and the Working Group on Coupled Modelling, the former coordinating body of CORDEX and responsible panel for CMIP5 are gratefully acknowledged. The Centre for Climate Change Research, Indian Institute of Tropical Meteorology, Pune, India, is acknowledged for providing CORDEX South Asia data. Prof. Andrew Sturman, University of Canterbury, New Zealand is acknowledged for improving the language of this manuscript.

Author contribution SB and SM: conceptualization, data analyses, manuscript writing. VG and APD: conceptualization, results verification and manuscript correction.

Funding SM received research project grant from NMHS, MoEFCC, GOI, (NMHS-2017-18/MG-02/478), for this work.

Data availability The World Climate Research Programme's Working Group on Regional Climate, and the Working Group on Coupled Modelling, former coordinating body of CORDEX and responsible panel for CMIP5 are gratefully acknowledged. The CORDEX data was obtained from Centre for Climate Change Research, Indian Institute of Tropical Meteorology, Pune, India.

Code availability The data analysis codes are available from SB and SM and can be shared after necessary approval from Competent Authority of GBPNIHE, India.

Declarations

Ethics approval and consent to participate Not applicable

Consent for publication Consents for publication from all the co-authors are received.

Conflict of interest The authors declare no competing interests.

References

Beniston M (2003) Climate change in mountain regions: a review of possible impacts. Clim Chang 59(1):5–31

Bhutiyani M, Kale V, Pawar N (2007) Long-term trends in maximum, minimum, and mean annual air temperatures across the northwestern Himalaya during the 20th century. Clim Chang 85:159–177

Bookhagen B, Burbank D (2006) Topography, relief, and TRMM-derived rainfall variations along the Himalaya. Geophys Res Lett 33:L08405. https://doi.org/10.1029/2006GL026037

Chalise S, Khanal N (2001) Rainfall and related natural disasters in Nepal. In: Tianchi Li, Chalise S, Upreti BN (eds) Landslide hazards, mitigation to the Hindukush-Himalayas ICIMOD, Nepal

Dash S, Sharma N, Pattnayak K, Gao X, Shi Y (2012) Temperature and precipitation changes in the north-east India and their future projections. Glob Planet Chang 98:31–44

Dhar O, Rakhecha P (1981) The effect of elevation on monsoon rainfall distribution in the central Himalayas. In: Lighthill J, Pearce RP (eds) Monsoon dynamics. Cambridge University Press, Cambridge

Dikshit KR, Dikshit JK (2014) North-east India: Land people and economy. Springer, Netherlands

Dimri AP (2006) Surface and upper air fields during extreme winter precipitation over the western Himalayas. Pur Appl Geophys 163(8):1679–1698

Dimri AP (2014) Sub-seasonal interannual variability associated with the excess and deficit Indian winter monsoon over the Western Himalaya. Clim Dyn 42(7-8):1793–1805

Dimri AP, Niyogi D (2013) Regional climate model application at subgrid scale on Indian winter monsoon over the western Himalayas. Int J Climatol 33(9):2185–2205. https://doi.org/10.1002/joc.3584

Dimri AP, Niyogi D, Barros A, Ridley J, Mohanty UC, Yasunari T, Sikka D (2015) Western disturbances: A review. Rev Geophys 53:225–246

Dimri AP, Kumar D, Choudhary A, Maharana P (2018) Future changes over the Himalayas: Mean temperature. Glob Planet Chang 162:235–251. https://doi.org/10.1016/j.gloplacha.2018.01.014

Dyurgerov MB, Meier MF (2005) Glaciers and the changing earth system: a 2004 snapshot, vol 58 Institute of Arctic and Alpine Research, University of Colorado Boulder, USA

Ghimire S, Choudhary A, Dimri AP (2015) Assessment of the performance of CORDEX-South Asia experiments for monsoonal precipitation over the Himalayan region during present climate: part I. Clim Dyn. https://doi.org/10.1007/s00382-015-2747-2

Giorgi F, Bi X, Pal J (2004) Mean, interannual variability and trends in a regional climate change experiment over Europe. II: climate change scenarios (2071-2100). Clim Dyn 23(7–8):839–858

Giorgi F, Bates GT (1989) The climatological skills of a regional model over complex terrain. Mon Weather Rev 117(11):2325–2347

Goyal M, Singh V, Meena A (2015) Geospatial and hydrological modeling to assess hydropower potential zones and site location over rainfall dependent inland catchment. Water Res Manag 29:2875–2894. https://doi.org/10.1007/s11269-015-0975-1

Hatwar H, Yadav BP, Rama Rao YV (2005) Prediction of western disturbances and associated weather over Western Himalaya. Curr Sci 88:913–920

IPCC (2014) Impacts, adaptation and vulnerability. Part B: regional aspects. Contribution of working gropu II to the fifth assessment report of IPCC Tech, Rep., Cambridge University Press

Kanwal M, Mukherjee S, Joshi R, Rai S (2019) Impact assessment of changing environmental and socio-economic factors on crop yields of central Himalaya with emphasis to climate change. Environ Ecol 37(1B):324–332

Kulkarni A, Patwardhan S, Krishna Kumar S, Karamuri A, Krishnan R (2013) Projected climate change in the Hindu Kush-Himalayan region by using the high-resolution regional climate model PRECIS. Mt Res Dev 33:142–151

Kumar P, Wiltshire A, Mathison C, Asharaf S, Ahrens B, Lucas-Picher P, Jacob D et al (2013) Downscaled climate change projections with uncertainty assessment over India using a high-resolution multimodel approach. Sci Total Environ 468:S18–S30

Maharana P, Dimri AP (2014) Impact of initial and boundary conditions on regional winter climate over Western Himalayas: a fixed domain size experiment. Glob Planet Chang 114:1–13

Mall R, Gupta A, Singh R, Singh R, Rathore L (2006) Water resources and climate change:An Indian perspective. Curr Sci 90(12):1610–1626

McGregor J, Dix M (2001) The CSIRO conformal-cubic atmospheric GCM. IUTAM symposium on advances in mathematical modeling of atmospheric and ocean dynamics pp 197–202

Midhuna T, Dimri A (2019) Future projection of winter precipitation over northwest India and associated regions using CORDEX-SA experiments. Theor Appl Climatol. https://doi.org/10.1007/s00704-019-03049-7

Mishra V (2015) Climatic uncertainty in Himalayan water towers. J Geophys Res. https://doi.org/10.1002/2014JD022650

Mukherjee S, Shukla R, Mittal A, Pandey A (2011) Mathematical analysis of a chaotic model in relevance to monsoon ISO. Met Atmos Phys 114:83–93

Mukherjee S (2017) Contrasting predictability of summer monsoon rainfall ISOs over the northeastern and western Himalayan region: an application of Hurst exponent. Meteorol Atmos Phys. https://doi.org/10.1007/s00703-017-0551-8

Mukherjee S, Joshi R, Prasad R, Vishvakarma S, Kumar K (2015) Summer monsoon rainfall trends in the Indian Himalayan region. Theor Appl Climatol 121(3-4):789–802. https://doi.org/10.1007/s00704-014-1273-1

Mukherjee S, Ballav S, Soni S, Kumar K, De UK (2016) Investigation of dominant modes of monsoon ISO in the northwest and eastern Himalayan region. Theor Appl Climatol 125(3-4):489–498. https://doi.org/10.1007/s00704-015-1512-0

Mukherjee S, Hazra A, Kumar K, Nandi S, Dhyani P (2019) Simulated projection of ISMR over Indian Himalayan region: assessment from CSIRO-CORDEX South Asia experiments. Meteorol Atmos Phys 131(1):63–79. https://doi.org/10.1007/s00703-017-0547-4

Mukherjee S, Gosavi V, Joshi R, Kumar K (2020) Impact of Nino phases on the summer monsoon of northwestern and eastern Himalaya. In: Himalayan weather and climate and their impact on the environment. Springer Nature. https://doi.org/10.1007/978-3-03029684-1_2

Mukherjee S (2021) Nonlinear recurrence quantifications of the monsoon-season heavy rainy-days over northwest Himalaya for the baseline and future periods. Sci Total Environ 789(7):147754. https://doi.org/10.1016/j.scitotenv.2021.147754

Nageshwararao M, Mohanty U, Ramakrishna S, Nair A, Kiran Prasad S (2016) Characteristics of winter precipitation over northwest India using high-resolution gridded dataset (1901-2013). Glob Planet Chang 147:67–85. https://doi.org/10.1016/j.gloplacha.2016.10.017

Nandargi A, Dhar O (2011) Extreme rainfall events over Himalaya between 1871 and 2007. Hydro Sci J 56(6):930–945

Palazzi E, Hardenber J, Terzago S, Provenzale A (2013) Precipitation in the Hindukush-Karakoram Himalaya: Observation and future scenarios. J Geophys Res - Atmos 118:85–100. https://doi.org/10.1029/2012JD018697

Parthasarathy B, Munot A, Kothawale D (1994) All-India monthly and seasonal rainfall series: 1871-1993. Theor Appl Climatol 49:217–224

Pattanaik D, Rajeevan M (2010) Variability of extreme rainfall events over India during southwest monsoon season. Meteorol Appl 17:88–104

Pisharoty P, Desai B (1956) Western disturbances and Indian weather. Mausam 7:333–338

Pohl B, Macron C, Monerie PA (2017) Fewer rainy days and more extreme rainfall by the end of the century in South Africa. Sci Rep 7:46466. https://doi.org/10.1038/srep46466

Rummukainen M (2010) State-of-the-art with regional climate models. Wiley Interdiscip Rev Clim Chang 1(1):82–96

Sanjay J, Krishnan R, Shrestha A, Rajbhandari R, Ren GY (2017) Downscaled climate change projections for the Hindu Kush Himalayan region using CORDEX South Asia regional climate models. Adv Clim Chang Res 8(3):185–198. https://doi.org/10.1016/j.accre.2017.08.003

Sen P (1968) Estimates of the regression coefficient based on Kendall's tau. J Amer Stat Assoc 39:1379–1389

Singh SP, Khadka BI, Karky B, Sharma E (2011) Climate change in the Hindu Kush Himalaya: the state of current knowledge. ICIMOD, Nepal

Solman SA, Nunez MN, Cabre MF (2008) Regional climate change experiments over southern South America. I: present climate. Clim Dyn 30(5):533–552

Wiltshire A (2014) Climate change implications for the glaciers of the Hindu Kush, Karakoram and Himalayan region. Cryosphere 8:941–958. https://doi.org/10.5194/tc-8-941-2014

Yadav R (2009) Role of equitorial central Pacific and northwest of North Atlantic 2-meter surface temperature in modulating Indian summer monsoon variability. Clim Dyn 32(4):549–563. https://doi.org/10.1007/s00382-008-0410-x

Yatagai A, Arakawa O, Kamiguchi K, Kawamoto H, Nodzu M, Hamada A (2009) A 44-year daily gridded precipitation dataset for Asia based on a dense network of rain gauges. Sci Online Lett Atmos 5:137–140

Yatagai A, Kamiguchi K, Arakawa O, Hamada A, Yasutomi N, Kitoh A (2012) APHRODITE: Constructing a long-term daily gridded precipitation dataset for Asia based on a dense network of rain gauges. Bul Amer Meteorol Soc 93:1401–1415

Publisher's note Springer Nature remains neutral with regard to jurisdictional claims in published maps and institutional affiliations.